Spectroscopic, Magnetic, and Electrochemical Studies of a Dimeric *N*-Substituted-Sulfanilamide Copper(II) Complex. X-ray and Molecular Structure of the Cu_2(sulfathiazolato)$_4$ Complex

Javier Casanova, Gloria Alzuet, Julio Latorre, and Joaquín Borrás*

Departamento de Química Inorgánica, Universidad de Valencia, Avenida Vicent Andrés Estellés, s/n, 46100 Burjassot, Valencia, Spain

Received August 8, 1996[⊗]

A copper(II) complex of formula $Cu_2(stz)_4$ (stz^- = sulfathiazolato) has been synthesized and characterized by single-crystal X-ray diffraction. The compound crystallizes in the orthorhombic system, space group $P2_1cn$ with $a = 10.595(7)$ Å, $b = 14.274(3)$ Å, $c = 29.65(1)$ Å, and $Z = 4$. The structure consists of dinuclear copper(II) units which contain four sulfathiazolato ligands bridging the metal ions through a nonlinear NCN group. The copper atoms are four-coordinated, the chromophore being CuN_4. The Cu···Cu bond distance is 2.671(2) Å. Magnetic susceptibility data in the temperature range 7−300 K show the occurrence of intramolecular antiferromagnetic coupling with $2J = -61.5$ cm^{-1}. This low exchange energy value has been analyzed and rationalized through extended Hückel calculations. EPR spectra at X- and Q-band frequencies show the signals corresponding to a dinuclear entity, being the zero-field splitting parameter, $D = 0.230$ cm^{-1}.

Introduction

Sulfanilamide and its N-substituted derivatives are well-known antibacterial drugs. The metal complexes of these substances have been extensively studied.[1−7] From the spectroscopic properties of the compounds, Bult[8] has suggested that the drugs behave as bidentate ligands through the $N_{sulfonamido}$ and the $N_{heterocyclic}$ atoms.

We have undertaken several studies on the characterization of some N-substituted sulfanilamide derivatives, mainly the sulfathiazole (Hstz) (Figure 1).

Until our research, no crystal structures of sulfathiazole metal complexes have been reported. In previous papers[9−13] we have obtained crystal structures of copper(II) and zinc(II) sulfathiazole compounds. In our study about the behavior as ligand of the Hstz, we found different forms of interaction with the metals. As a neutral ligand, the Hstz acts as monodentate, binding the metal ion through the N_{amino} atom.[10,11] As a deprotonated ligand, stz^- has a variety of coordination behavior, in the $[Zn(stz)_2]\cdot H_2O$ complex, it binds to one Zn(II) through the N_{amino} and to another Zn(II) through the $N_{thiazole}$ atom in a polymeric structure;[9] in the $[Cu(stz)(py)_3Cl]$ compound, the anionic ligand binds to the Cu(II) through the $N_{thiazole}$ atom,[12] and in the $[Cu(stz)_2(Him)_2]\cdot$MeOH and $[Cu(stz)_2(mim)_2]\cdot H_2O$ complexes, one of the stz^- exhibits bidentate behavior linking the metal ion through the $N_{thiazole}$ and the $N_{sulfonamido}$ atoms.[13]

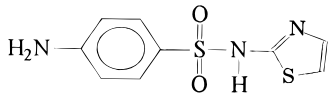

Figure 1. Sulfathiazole.

Here, we report a binuclear copper complex. To our knowledge, this compound is the first structurally characterized example of a dimer of sulfathiazole with the ligand bridging the two copper ions through the $N_{thiazole}$ and $N_{sulfonamido}$ atoms.

The $Cu_2(stz)_4$ complex is a dimer one, classified in the type IV of copper dimers[14] with triatomic NCN bridging groups. An interesting aspect of the ligand in this compound is the presence of a nonlinear bridging NCN, also found in molecules of biological importance like adenine,[15−20] and that provides an efficient pathway for coupling magnetism. Considerable attention has focused on the bridging capabilities of a closely related system containing the NCN group such as the copper complexes of the adenine. The synthesis of these dimers is important for studying by magnetic and spectroscopic techniques the nature of the spin−spin interactions which occur intramolecularly between the metal atoms.

* Author to whom correspondence should be addressed.

[⊗] Abstract published in *Advance ACS Abstracts,* April 1, 1997.

(1) Bult, A. *Pharm. Weekbl., Sci. Ed.* **1981**, *3*, 1.
(2) Bult, A. Metal Complexes of Sulfanilamides. In *Metal Ions in Biological Systems*; Sigel, Ed.; Dekker: New York, 1983; Vol. 16.
(3) Narang, K. K.; Gupta, J. K. *Transition Met. Chem. (London)* **1977**, *2*, 83.
(4) Narang, K. K.; Gupta, J. K. *Transition Met. Chem. (London)* **1977**, *2*, 181.
(5) Malecki, F.; Staroscik, R.; Weiss-Gradzinska, W. *Pharmazie* **1984**, *39*, 158.
(6) Pezeshk, A.; Pezeshk, V. *J. Inorg. Biochem.* **1990**, *38*, 185.
(7) Bonamartini Corradi, A.; Gozzoli, E.; Menabue, L.; Saladini, M.; Battaglia, L. P.; Sgarabotto, P. *J. Chem. Soc., Dalton Trans.* **1994**, 273.
(8) Bult, A.; Uitterdijk, J. D.; Klasen, H. B. *Transition Met. Chem. (London)* **1979**, *4*, 285.
(9) Casanova, J.; Alzuet, G.; Ferrer, S.; Borrás, J.; García-Granda, S.; Perez-Carreño, E. *J. Inorg. Biochem.* **1993**, *51*, 689.
(10) Casanova, J.; Alzuet, G.; Borrás, J.; Amigó, M.; Debardemaeker, T. *Z. Kristallogr.* **1993**, *209*, 271.
(11) Casanova, J.; Alzuet, G.; Borrás, J.; Timoneda, J.; García-Granda, S.; Cándano-García, I. *J. Inorg. Biochem.* **1994**, *56*, 65.
(12) Casanova, J.; Alzuet, G.; Borrás, J.; Latorre, J.; Sanaú, M.; García-Granda, S. *J. Inorg. Biochem.* **1995**, *60*, 219.
(13) Casanova, J.; Alzuet, G.; Borrás, J.; Carugo, O. *J. Chem. Soc., Dalton Trans.* **1996**, 2239.
(14) Hathaway, B. J. Copper. In *Comprehensive Coordination Chemistry*; Wilkinson, G., Gillard, R. D., Cleverty, J. A., Eds.; Pergamon Press: New York, 1987; Vol. 5.
(15) Sletten, E. *Acta Crystallogr.* **1969**, *B25*, 1480.
(16) de Meester, P.; Goodgame, D. M. L.; Angela Price, K.; Skapski, A. C. *Nature* **1971**, *229*, 191.
(17) de Meester, P.; Skapski, A. C. *J. Chem. Soc. A* **1971**, 2167.
(18) Terzis, A.; Beauchamp, A. L.; Rivest, R. *Inorg. Chem.* **1973**, *12*, 1170.
(19) Brookes, R. W.; Martin, R. L. *Inorg. Chem.* **1975**, *14*, 528.
(20) Sonnenfroh, D.; Kreilick, R. W. *Inorg. Chem.* **1980**, *19*, 1259.

S0020-1669(96)00968-8 CCC: $14.00

Experimental Section

Materials. Copper fluoride dihydrate and sulfathiazole were reagents of grade and used without purification. Analytical data (C, H, N) were obtained in a Carlo Erba Instrument Model MOG 1106 of the Inorganic Chemistry Department of the University of Salamanca (Spain). The copper content was determined by atomic absorption spectroscopy.

Synthesis of the Complex. A methanolic solution (25 mL) containing copper(II) fluoride (0.10 g, 1 mmol) was added to a warm methanolic solution (50 mL) containing Nastz (0.55 g, 2 mmol) with continuous stirring. The solution became dark blue, and immediately a purple precipitate was obtained. The solid was filtered off and was dried (yield: 90%). Single crystals were obtained through the diffusion method. Anal. Calcd for $C_{36}H_{32}Cu_2N_{12}O_8S_8$: C, 37.78%; H, 2.82%; N, 14.69%; Cu, 11.10%. Found: C, 37.10%; H, 2.90%, N, 14.41%; Cu, 11.32%. Selected IR bands (KBr cm^{-1}): 3480m, 3390m, NH; 1500m, thiazole ring; 1320s, 1130s, 550−570s, SO_2. It should be pointed out that when other copper (II) salts (chloride, nitrate, perchlorate, etc.) were used, the same dinuclear compound is obtained, but only single crystals suitable for X-ray diffraction measurements were formed with copper(II) fluoride.

Physical Techniques. IR spectra were recorded on a Perkin-Elmer 843 instrument. Samples were prepared using the KBr technique. Vis−UV spectra was recorded on a Perkin-Elmer Lambda 15 spectrophotometer. EPR spectra of ground crystals were carried out at X-band frequencies with a Bruker ER 200D spectrometer and at Q-band frequencies with a Bruker-ESP300 equipped with an Oxford continuous-flow cryostat. Room-temperature EPR spectra of copper complex solutions were taken in a flat cell purchased from Wilmad Glass Co. Magnetic susceptibility measurements were carried out in the 7−300 K temperature range with a fully automatized AZTEC DSM8 pendulum-type susceptometer equipped with a TBT continuous-flow cryostat and a Bruker BE15 electromagnet, operating at 1.8 T. Mercury tetrakis-(thyocianato)cobaltate(II) was used as a susceptibility standard. Corrections for the diamagnetism of the complex was estimated from Pascal's constants to -562×10^{-6} emu. Magnetic susceptibility data were also corrected for temperature-independent paramagnetism [60 $\times 10^{-6}$ emu/Cu(II)] and magnetization of the sample holder.

Electrochemical measurements were carried out in a three-electrode cell; the working and auxiliary electrodes were platinum, and the reference one was a saturated calomel electrode (SCE) electrically connected to the solution via a "salt bridge" containing a saturated solution of supporting electrolyte and the solvent. Cyclic voltammograms were obtained with a BAS potentiostat Model CV-27 and recorded on a Omnigraphic 100 recorder.

X-ray Crystal Structure Determination. A red-purple well-formed crystal was of approximate size 0.15 × 0.10 × 0.15 mm. Mo Kα radiation monochromated with a graphite crystal was used on an Enraf-Nonius CAD-4 single-crystal diffractometer (λ = 0.170 73 Å). The unit-cell dimensions were determined from the angular settings of 25 reflections with θ between 15 and 25°. The space group was $P2_1cn$. A set of 4419 reflections was measured, in the *hkl* range (0, 0, 0) to (12, 16, 35) between θ limits: $1 < \theta < 25°$. The $\omega-2\theta$ scan technique and a variable scan rate with a maximum scan time of 60 s/reflection were used. The intensity of the primary beam was checked throughout the data collection by monitoring three standard reflections every 3600 s. The final drift correction factors were between 0.97 and 1.01. On all reflections profile analysis was performed.[21,22] Some double measured reflections were averaged: 4145 "unique" reflections from which were 3243 with $F_o > 4\sigma(F_o)$. Lorentz and polarization corrections were applied, and the data were reduced to $|F_o|$ values. The structure was solved by the Patterson method using the program SHELXS86.[23] Isotropic least-squares refinement was performed by means of SHELXS93,[24] converging to R = 0.095. At this stage additional empirical absorption correction was applied using DIFABS.[25] The maximum and minimum absorption correction factors were respectively 1.07 and 0.92. Hydrogen atoms were geometrically placed.

Table 1. Crystallographic Data for the $Cu_2(stz)_4$ Complex

formula	$C_{36}H_{32}Cu_2N_{12}O_8S_8$	cryst size (nm)	0.15 × 0.10 × 0.15
fw	1144.3	μ(Mo Kα) (cm^{-1})	32.30
space group	$P2_1cn$	λ(Mo Kα) (Å)	0.710 73
a (Å)	10.595(7)	orientation reflcns number	25
b (Å)	10.274(3)	range (deg)	$15 < \theta < 25$
c (Å)	29.65(1)	data collcn range (deg)	$1 < \theta < 25$
Z	4	no. of unique data	4145
V (Å^3)	4483(4)	total with $F_o > 4\sigma(F_o)$	3243
F(000)	2776	R_1[a]	0.035
D_c (g·cm^{-3})	1.695	R_{w2}[b]	0.1086

[a] $R_1 = \sum||F_o| - |F_o||/\sum|F_o|$. [b] $R_{w2} = \sum\omega(F_o^2 - F_c^2)^2/\omega(F_o^2)^2$. $\omega = 1/[\sigma^2(F_o^2) + (0.1000P)$; $P = [(\max(F_o^2,0) + 2(Fc)_2]/3$.

During the final stages of the refinement the positional parameters and the anisotropic thermal parameters of the non-hydrogen atoms were refined. The hydrogen atoms were isotropically refined with a common thermal parameter. The final conventional agreement factors were R_1 = 0.035 and R_{w_2} = 0.1086 for the 3243 "observed" reflections and 631 parameters. The maximum shift to the estimated standard deviation (esd) ratio in the last full matrix least squares cycle was 0.01. The final difference Fourier map showed no peaks higher than 0.49 e·A^{-3} nor deeper than 0.62 e·A^{-3}. Atomic scattering factors were taken from *International Tables for X-ray Crystallography*.[26] The crystallographic plots were made with ORTEP.[27] All calculations were made on an IBM PS Pentium computer. All crystallographic details are listed in Table 1.

Results and Discussion

Description of the Structure. Final atomic coordinates for all non-hydrogen atoms are listed in Table 2. Figure 2 shows an ORTEP drawing of the structure of the dimer unit with the atomic numbering scheme. Selected bond distances and angles are collected in Table 3. The structure consists of dimer units which contain stacking interactions between the aromatic rings and tridimensionally connected by means of hydrogen bonds (see Figure 3).

Each copper atom of the dinuclear species [Cu1 and Cu2] is four-coordinated, with a slightly distorted square-planar environment: the Cu1 is linked to N1 and N8 thiazole nitrogen atoms from two sulfathiazolato ligands and N2 and N3 sulfonamido nitrogen atoms from the other two sulfathiazolato anions; the Cu2 is bonded to N5 and N6 of the thiazole rings and N4 and N7 of the sulfonamido groups. The metal−ligand distances $Cu-N_{thiazole}$ are in the range from 1.93 to 1.98 Å, and the $Cu-N_{sulfonamido}$ ones are in the range from 2.01 to 2.09 Å. These distances are similar to those observed in the previously reported sulfathiazole complexes.[9,11,13] The bond angles in both CuN_4 chromophores are nearly regular, ranging from 88 to 92°. In both chromophores, the N thiazole atoms are in the *trans* position. The deviations of N1, N2, N3, and N8 atoms from the mean plane $Cu1N_4$ are −0.124, +0.225, +0.218, and −0.125 Å, respectively, and the Cu1 is displaced −0.194 Å from this plane in the opposite direction to the other

(21) Lehman, M. S.; Larsen, F. K. *Acta Crystallogr.* **1974**, *A30*, 580.
(22) Grant, D. F.; Gabe, E. J. *J. Appl. Crystallogr.* **1978**, *11*, 114.
(23) Sheldrick, G. M. SHELX86. In *Crystallographic Computing 3*; Sheldrick, G. M., Kruger, C., Goddard, R., Eds.; Clarendon Press: Oxford, U.K., 1985.
(24) Sheldrick, G. M. *SHELXS-93, Program for Crystal Structure Refinement*; Institute für Anorganishe Chemie de Universitat: Göttingen, Germany, 1993.
(25) Walker, N.; Stuart, D. *Acta Crystallogr.* **1983**, *A39*, 158.
(26) *International Tables for X-ray Crystallography*; Kynoch Press: Birmingham, England, 1974; Vol. IV. Present distributor: Kluwer Academic Publishers, Dordrecht, The Netherlands,
(27) Johnson, C. K. ORTEP, Report ORNL-3794; Oak Ridge National Laboratory: Oak Ridge, TN, 1971.

Table 2. Atomic Coordinates ($\times 10^4$) and Equivalent Isotropic Displacement Parameters (Å^2 $\times$ 10^3) for $Cu_2(stz)_4$, with Their Esd's in Parentheses[a]

atom	*x*	*y*	*z*	*U*(eq)
Cu1	−429(1)	2091(1)	883(1)	33(1)
Cu2	1572(1)	1852(1)	1418(1)	36(1)
S1	−2606(2)	1003(1)	1235(1)	39(1)
S2	2660(2)	−109(2)	1300(1)	62(1)
S3	281(2)	3541(1)	170(1)	44(1)
S4	1992(2)	3690(1)	1935(1)	56(1)
S5	−1517(2)	723(2)	2255(1)	50(1)
S6	3350(2)	3173(2)	213(1)	51(1)
S7	−939(3)	4396(2)	1868(1)	66(1)
S8	1494(3)	−361(1)	254(1)	66(1)
N1	−977(6)	3119(4)	1263(2)	43(1)
N2	−1140(5)	1201(4)	1358(2)	38(1)
N3	926(5)	2934(4)	562(2)	36(1)
N4	992(6)	3202(4)	1596(2)	42(1)
N5	2699(6)	2360(4)	944(2)	40(1)
N6	506(6)	1336(4)	1880(2)	39(1)
N7	1619(6)	575(4)	1082(2)	44(1)
N8	223(6)	1034(3)	527(2)	37(1)
N9	342(11)	−2720(7)	2602(3)	90(3)
N10	−3181(8)	−3127(5)	1243(3)	63(2)
N11	3805(8)	7078(5)	982(3)	60(2)
N12	696(8)	7488(5)	759(3)	75(2)
O1	−3438(6)	1393(4)	1569(2)	54(1)
O2	−2698(5)	1354(4)	779(2)	50(1)
O3	3201(9)	−698(6)	966(3)	113(3)
O4	3472(7)	508(6)	1563(3)	110(3)
O5	−1022(6)	3247(4)	202(2)	63(2)
O6	937(6)	3429(4)	−256(2)	59(2)
O7	1392(8)	3994(4)	2345(2)	78(2)
O8	2984(8)	2988(4)	1963(2)	83(2)
C10	−2798(7)	−217(5)	1235(2)	37(2)
C11	−2275(8)	−742(5)	884(2)	46(2)
C12	−2435(9)	−1707(5)	890(3)	52(2)
C13	−3085(8)	−2165(5)	1238(3)	50(2)
C14	−3580(8)	−1601(5)	1577(2)	49(2)
C15	−3458(8)	−648(5)	1580(2)	51(2)
C20	1914(7)	−828(5)	1697(2)	43(2)
C21	645(8)	−1014(5)	1682(3)	49(2)
C22	123(9)	−1626(6)	1990(3)	57(2)
C23	852(9)	−2069(6)	2319(3)	56(2)
C24	2127(10)	−1849(6)	2328(3)	58(2)
C25	2660(9)	−1254(5)	2025(3)	56(2)
C30	375(8)	4726(5)	322(2)	45(2)
C31	1328(7)	5315(5)	136(3)	49(2)
C32	1386(8)	6229(6)	272(3)	55(2)
C33	624(8)	6572(5)	614(3)	54(2)
C34	−289(9)	5977(5)	803(3)	54(2)
C35	−395(8)	5068(5)	648(2)	47(2)
C40	2594(8)	4696(5)	1656(3)	50(2)
C41	3513(9)	4634(6)	1328(3)	59(2)
C42	3922(8)	5406(5)	1112(3)	54(2)
C43	3418(7)	6295(5)	1204(2)	46(2)
C44	2477(8)	6345(5)	1531(2)	50(2)
C45	2044(8)	5564(5)	1758(2)	49(2)
C100	−690(6)	1128(5)	1789(2)	36(2)
C101	−167(9)	860(6)	2574(3)	61(2)
C102	795(9)	1175(6)	2333(3)	55(2)
C200	2212(7)	2823(4)	599(2)	35(1)
C201	4493(8)	2663(5)	546(3)	50(2)
C202	3993(8)	2256(5)	907(3)	46(2)
C300	−186(8)	3508(4)	1560(2)	45(2)
C301	−2327(10)	4219(6)	1578(3)	67(3)
C302	−2178(8)	3507(6)	1286(3)	54(2)
C400	1109(7)	461(5)	670(2)	41(2)
C401	382(10)	98(7)	−104(3)	66(2)
C402	−164(7)	836(5)	87(2)	44(2)

[a] *U*(eq) is defined as one-third of the trace of the orthogonalized $\mathbf{U}_{ij}$ tensor.

$Cu2-N_4$ plane. The deviations of N4, N5, N6, and N7 atoms from the mean plane $Cu2-N_4$ are −0.226, +0.154, +0.153, and −0.227 Å, respectively, and the Cu2 is displaced +0.146 Å from the mean plane in the opposite direction to the $Cu1-N_4$ plane. The dihedral angle between the two CuN_4 mean planes is 0.10°, indicating a parallel arrangement. The very short Cu1···Cu2 distance [2.671(2) Å] appears to be primarily determined by the width of the "bite" of the bridging ligand. It is noteworthy that in spite of the Cu1 and Cu2 atoms being placed below and above the $Cu1-N_4$ and $Cu2-N_4$ mean planes, the metal−metal distance is very short, comparable with the shortest Cu···Cu distances found in copper−adenine complexes.[15−20]

Tetrahedrality for any tetracoordinate copper complex can be characterized from the angle subtended by two planes, each encompassing the copper and two adjacent donor atoms.[28] For strictly square-planar complexes with D_{4h} symmetry, the tetrahedrality is 0°. For tetrahedral complexes with D_{2d} symmetry, the tetrahedrality equals 90°. The values of these dihedral angles for $Cu_2(stz)_4$ are 14 and 11°, respectively, suggesting a slight distortion from a square-planar geometry.

The sulfathiazolato anions act as a bridge linking to one Cu(II) ion through the $N_{thiazole}$ atom and to the other Cu(II) by means of the $N_{sulfonamido}$ atom. It must be noted that the bridge NCN formed by each of the four ligands is very unusual. The internal geometry of the sulfathiazole ligand is normal and agrees with numerous studies performed previously.[9,12,29,30]

Crystal Packing. The dimer units are stabilized by two weak stacking interactions between the thiazole [C100−S5−C101−C102−N6] and phenyl [C20−C21−C22−C23−C24−C25] rings (shortest distance 2.78 Å, angle between planes 25.9°) and between phenyl rings [C30−C31−C32−C33−C34−C35] and [C41−C42−C43−C44−C45] (shortest distance 3.23 Å, angle between plane 25.06°).

Dimer units are connected by weak hydrogen bonds involving the N_{amino} and the $O_{sulfonamido}$ atoms (see Table 4).

Infrared Spectrum. Previous studies on sulfathiazole complexes have shown that useful information on the mode of coordination of the ligand may be obtained from an examination of infrared spectra. The ν(N−H) vibrations at 3480 and 3390 cm^{-1} are shifted to higher frequencies with respect to the equivalent ones in the uncoordinated ligand (3320 and 3280 cm^{-1}). This shift is consistent with that observed for other metal−sulfathiazole complexes. The bands attributed to the SO_2 group that appear as sharp peaks at 1320, 1130, and 550−570 cm^{-1} (corresponding to ν_{as}, ν_s, and scissors and wagging vibrations, respectively) remain unchanged. According to the deprotonation and coordination of the ligand, the characteristic band of the thiazole ring at 1540 cm^{-1} in the free ligand is strongly reduced and shifted to lower frequencies (1500 cm^{-1}).

Electronic Spectrum. The reflectance diffuse spectrum shows a very broad and intense band centered around 19 000 cm^{-1}, characteristic of a CuN_4 chromophore with the metal ion in a distorted square-planar arrangement.[14] A linear correlation between the dihedral angle with the highest energy d−d transition in the electronic spectra of some CuN_4 chromophores has been reported.[31] From this correlation the maximum for a CuN_4 chromophore is at 19 960 cm^{-1} for a regular square-planar geometry. Taking into account the dihedral angles (11 and 14°) obtained by X-ray crystallography for $Cu_2(stz)_4$, the values of ν_{max} found from this approximation are 19 050 and 18 900 cm^{-1}

(28) Battaglia, L. P.; Bonamartini-Corradi, A.; Marcotrigiano, G.; Menabue, L.; Pellacani, G. C. *Inorg. Chem.* **1979**, *18*, 148.
(29) Kruger, G. J.; Garner, G. *Acta Crystallogr.* **1971**, *B27*, 326.
(30) Kruger, G. J.; Garner, G. *Acta Crystallogr.* **1972**, *B28*, 272.
(31) Ravichandran, V.; Chacko, K. K.; Aoki, A.; Yamazaki, H.; Ruiz-Sanchez, J.; Suarez-Verela, J.; Lopez-Gonzalez, J. D.; Salas-Peregrin, J. M.; Colacio-Rodriguez, E. *Inorg. Chim. Acta* **1990**, *173*, 107.

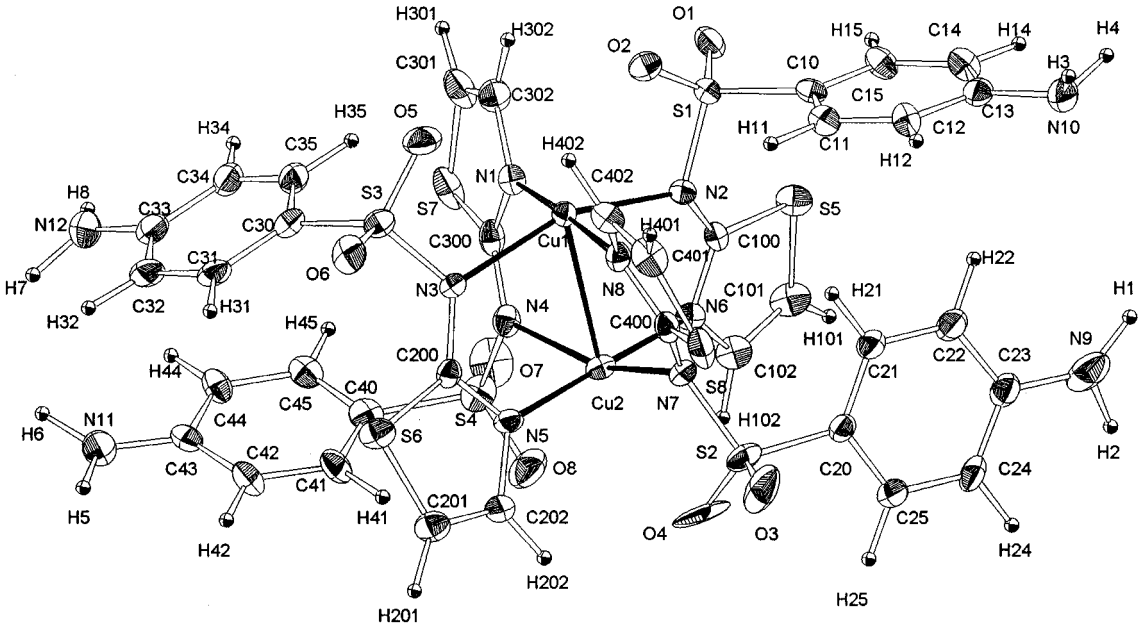

Figure 2. ORTEP drawing of the $Cu_2(stz)_4$ molecule. Thermal ellipsoids are drawn at the 25% probability level.

Table 3. Selected Bond Lengths (Å) and Angles (deg) for $Cu_2(stz)_4$

Cu1−N1	1.938(6)	Cu1−N8	1.967(5)
Cu1−N2	2.041(5)	Cu1−N3	2.100(6)
Cu1−Cu2	2.671(2)	Cu2−N6	1.922(5)
Cu2−N5	1.982(6)	Cu2−N4	2.090(6)
Cu2−N7	2.077(6)		
N1−Cu1−N8	176.0(3)	N1−Cu1−N2	87.6(2)
N8−Cu1−N2	91.3(2)	N1−Cu1−N3	91.9(2)
N8−Cu1−N3	87.6(2)	N2−Cu1−N3	157.1(2)
N1−Cu1−Cu2	89.4(2)	N8−Cu1−Cu2	86.7(2)
N2−Cu1−Cu2	78.6(2)	N3−Cu1−Cu2	78.5(2)
N6−Cu2−N5	178.7(3)	N6−Cu2−N4	90.1(2)
N5−Cu2−N4	91.0(2)	N6−Cu2−N7	91.1(2)
N5−Cu2−N7	88.1(2)	N4−Cu2−N7	159.5(2)
N6−Cu2−Cu1	90.4(2)	N5−Cu2−Cu1	90.5(2)
N4−Cu2−Cu1	78.4(2)	N7−Cu2−Cu1	81.1(2)

for the Cu1−N_4 and Cu2−N_4 chromophores, respectively, which agree well with the experimental results.

Electrochemistry. The electrochemical properties of the dinuclear compound were studied by cyclic voltammetry in 10^{-3} M acetone solution containing 0.1 M NBu_4PF_6 as supporting electrolyte in the potential range from +1.0 to −1.5 V vs saturated calomel electrode (SCE) (Figure 4a).

The cyclic voltammograms involve two clearly distinguishable redox processes corresponding to two well-defined one-electron reduction irreversible peaks A_1 (−0.05 V) and A_2 (−0.37 V) that tentatively can be assigned as follows:

$$Cu^{II}Cu^{II} \xrightarrow{-0.05\ V} Cu^{II}Cu^{I} \xrightarrow{-0.37\ V} Cu^{I}Cu^{I}$$

If the sweep is reversed after peak A_2 is scanned, A'_2 (0.40 V) and A'_1 (0.75 V) peaks are observed, so $\Delta Ep_1 = Ep(A'_1) - Ep(A_1)$ and $\Delta Ep_2 = Ep(A'_2) - Ep(A_2)$ are 0.80 and 0.77 V, respectively. According to that, the Cu^I-Cu^I species generated after reduction in A_2 are unstable, probably due to the dissociation of the copper−copper bond. Tentatively, we can assume that A'_2 and A'_1 peaks correspond to the oxidation of mononuclear species from Cu^0 to Cu^I and from Cu^I to Cu^{II}, respectively. The formation of the Cu^0 is clearly observed in the voltammogram of the title compound in MeCN (Figure 4b). The picture shows two reduction peaks like the previous voltammogram in acetone, and the reverse scan shows a characteristic reoxidation stripping peak A'_2 (−0.11 V) of the Cu^0 species.

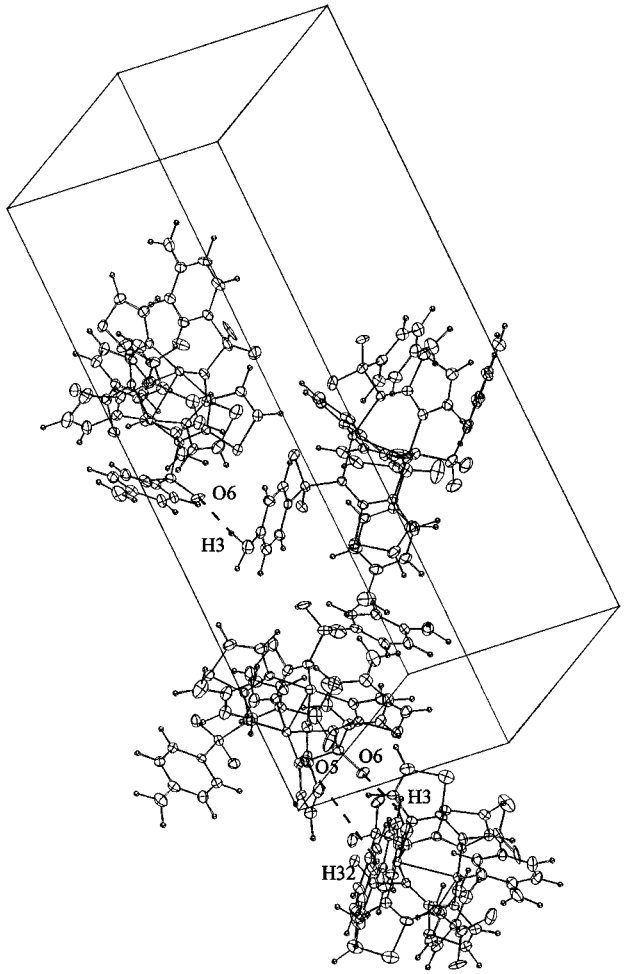

Figure 3. Crystal packing of the $Cu_2(stz)_4$ complex showing the stacking interactions and the hydrogen bonds.

EPR Measurements. The dimetallic nature of the $Cu_2(stz)_4$ complex is also indicated by EPR data. The X- and Q-band EPR spectra taken on ground crystals at room temperature and

Table 4. Distances (Å) and Angles (deg) between the Atoms Involved in the Observed Hydrogen Bonds for the $Cu_2(stz)_4$ Complex

donor−H		donor···acceptor		H···acceptor		donor−H···acceptor	
N9−H2	1.080(0.015)	N9···O1[a]	3.046(0.012)	H2···O1[a]	2.104(0.012)	N9−H2···O1[a]	144.33(1.05)
N10−H3	1.080(0.012)	N10···O6[b]	3.101(0.010)	H3···O6[b]	2.105(0.010)	N10−H3···O6[b]	152.14(0.72)
N11−H5	1.080(0.012)	N11···O6[c]	3.205(0.011)	H5···O6[c]	2.128(0.010)	N11−H5···O6[c]	174.34(0.79)
N11−H6	1.080(0.011)	N11···O3[d]	3.236(0.012)	H6···O3[d]	2.193(0.012)	N11−H6···O3[d]	161.76(0.85)

[a] $(x + {}^1/_2, y - {}^1/_2, -z + {}^1/_2)$. [b] $(x - {}^1/_2, -y, -z)$. [c] $(x + {}^1/_2, -y + 1, -z)$. [d] $(x, y + 1, z)$.

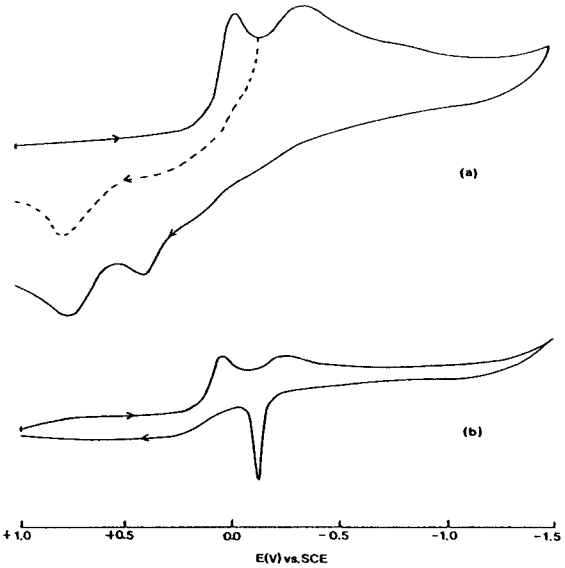

Figure 4. Cyclic voltammograms in the scan range +1.0 to −1.5 V for $Cu_2(stz)_4$ in acetone solution (a) at a scan rate of 0.15 $V \cdot s^{-1}$ and in acetonitrile solution (b) at a scan rate of 0.05 $V \cdot s^{-1}$.

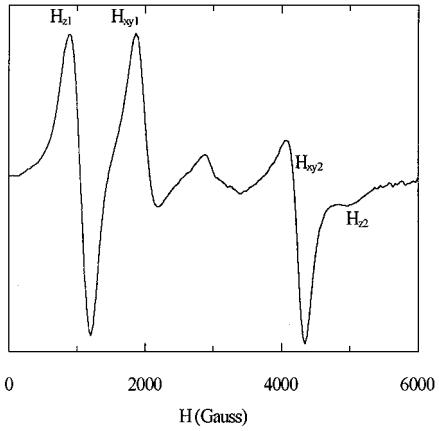

Figure 5. X-band EPR spectrum of the $Cu_2(stz)_4$ complex at room temperature.

100 K, respectively, are shown in Figures 5 and 6. Solution of the spin Hamiltonian for the triplet state of dimetallic copper complexes is given by

$$H = g\beta BS + DS_{z2} + E(S_{x2} - S_{y2}) - 2D/3$$

where D and E are zero-field splitting parameters. As shown by Wasson et al.,[32] two allowed transitions by the selection rule ($\Delta m_s = \pm 1$) will result in each principal direction, and six resonance fields can be determined. Furthermore a transition with ($\Delta m_s = \pm 2$) is also obtained. The six resonance fields are H_{x1}, H_{y1}, H_{z1}, H_{x2}, H_{y2}, and H_{z2} whose equations are proposed by Wasserman et al.[33] When D is lower than $h\nu$, as is usually

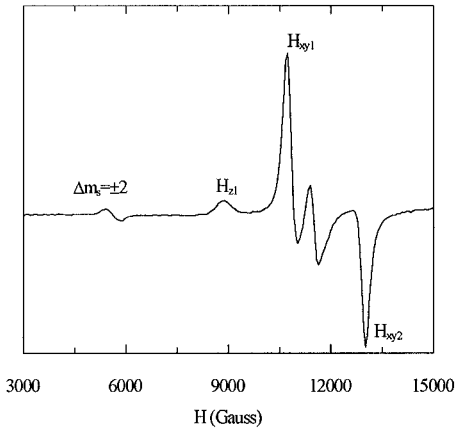

Figure 6. Q-band EPR spectrum of the $Cu_2(stz)_4$ complex at 100 K.

Table 5. EPR Data for the $Cu_2(stz)_4$ Complex[a]

	X-band	Q-band
$\Delta m_s = \pm 2$	*b*	5 595
H_{z1}	886	8 860
H_{xy1}	1873	10 715
H_{z2}	4900	*c*
H_{xy2}	4180	13 015

[a] Resonance fields in gauss (=10^{-4} T). [b] Not resolved from nearby $\Delta m_s = \pm 1$ band. [c] Hidden by stronger H_{xy2} band.

the case in compounds containing copper dimers, and $E = 0$, the solution of spin Hamiltonian yields four allowed ($\Delta m_s = \pm 1$) at resonance fields H_{z1}, H_{z2}, H_{xy1}, and H_{xy2} given by the equations

$$h\nu = D - g_{\parallel}\beta H_{z1}$$

$$h\nu = -D + g_{\parallel}\beta H_{z2}$$

$$h\nu = -D/2 + [D^2/4 - (g_{\perp}\beta H_{xy1})^2]^{1/2}$$

$$h\nu = -D/2 + [D^2/4 + (g_{\perp}\beta H_{xy2})^2]^{1/2}$$

In addition, the formally forbidden transition ($\Delta m_s = \pm 2$) the so-called half-field spin transition, is often observed. The position of the low-field edge of the half-field signal in a powder spectrum is given by the equation[34]

$$H_{\min}(\Delta m_s = 2) = {}^1/_2 g\beta[(h\nu)^2 - 4(D^2/3 + E^2)]^{1/2}$$

The observed transitions are summarized in Table 5, from these the calculated parameters are $g_{\parallel} = 2.33$, $g_{\perp} = 2.09$, and $D = 0.230$ cm^{-1}. The values of H_{z2} and H_{xy2} must be virtually coincident at the Q-band frequency, and consequently the low-intensity H_{z2} is hidden by the much stronger H_{xy2} band. Changing the microwave frequency to X-band enables a clear separation of these transitions to be made (Figure 5). Con-

(32) Wasson, J. R.; Chin-I Shyr; Trapp, C. *Inorg. Chem.* **1968**, *7*, 469.
(33) Wasserman, E.; Snyder, L. C.; Yager, W. A. *J. Chem. Phys.* **1964**, *41*, 1763.
(34) Eaton, S. A.; More, K. M.; Sawant, B. M.; Eaton, G. R. *J. Am. Chem. Soc.* **1983**, *105*, 6550.

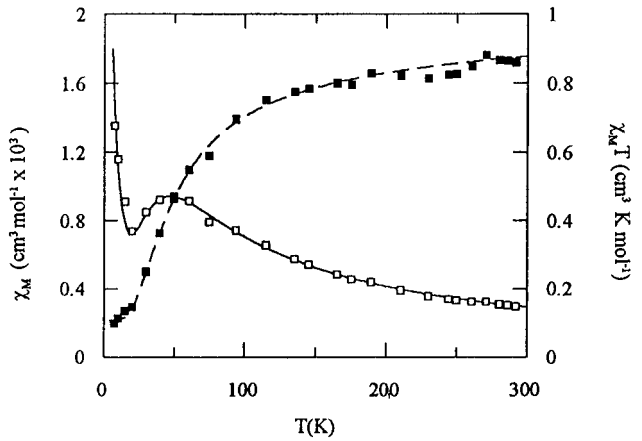

Figure 7. Plot of molar magnetic susceptibility (□) and $\chi_M T$ (■) for the $Cu_2(stz)_4$ compound as a function of temperature. The solid line represents the best fit to the data.

versely, the H_{z1}, H_{xy1}, and $\Delta m_s = \pm 2$ transitions could not have been unambiguously assigned from the X-band results alone because of appreciable band overlap at this frequency. However, these transitions are clearly resolved and readily assigned at Q-band frequency.

The D value observed ($=0.230$ cm^{-1}) is slightly higher than the range of D values reported for copper(II) dimers with nitrogen donor atoms in the bridges.[35]

In order to obtain more information about the monomeric copper(II) complex also present in a small amount in the sample, the purple complex was obtained in solid state doped in the diamagnetic matrix of the complex $[Zn(stz)_2]\cdot H_2O$. The EPR of the magnetically diluted complexes of copper(II) (Cu:Zn = 1:4 and 1:9) show clearly the anisotropic spectra of a monomeric copper(II) complex with an axial symmetry and the signals of the dimer weaker with respect to those observed in the EPR of the $Cu_2(stz)_4$ complex. The calculated EPR parameters of the monomer are $g_{\|} = 2.35$, $g_{\perp} = 2.07$, and $A_{\|} = 132 \times 10^{-4}$ cm^{-1}, suggesting a tetrahedral arrangement around the metal ion.[36] As the crystal structure of the $[Zn(stz)_2]\cdot H_2O$ was previously determined, we know that the Zn(II) ions is tetrahedrally surrounded by two $N_{thiazole}$ and two N_{amino}, so we suggest that the Cu(II) in the doped powder presents a coordination polyhedron similar to that of the Zn(II) and not the planar CuN_4 found in the dimer copper complex.

Solutions of the $Cu_2(stz)_4$ in MeOH−ethylene glycol (1:1) that have the same electronic spectrum as the reflectance one of $Cu_2(stz)_4$ exhibit an EPR spectrum at room temperature with an isotropic signal at 3230.4 G, giving a g_0 value of 2.16 and a half-signal at 1502.9 G, suggesting the existence of the dimer in this solution.

Magnetic Measurements. Susceptibility values per mole of dimer as a function of the temperature have been plotted in Figure 7. The dominant features of the data are a maximum near 50 K and a rapid decrease to zero at lower temperatures. An increase in susceptibility at the lowest temperatures of the type seen here is often observed in antiferromagnetically coupled copper complexes and has been accounted for by the presence of small amounts of paramagnetic impurities.[37] The solid curve in Figure 7 is the best fit of the data to the modified Bleaney−Bowers equation for the exchange coupled copper(II) dimers:

$$\chi_M = Ng^2\beta^2\{kT[3 + \exp(-2J/kT)]\}^{-1}(1 - \rho) + \rho Ng^2\beta^2/(4kT) + N\alpha$$

which results from a consideration of the eigenvalues of $H = -2JS_1S_2$, the Heisenberg exchange Hamiltonian for two interacting $S = {}^1/_2$ centers [χ_M is the molar magnetic susceptibility, $N\alpha$ is the temperature independent paramagnetism (60×10^{-6} emu/copper), and ρ is the fraction of monomeric impurity]. A nonlinear regression analysis of the data was carried out with ρ as a floating parameter. The best fit line shown in Figure 7 is for $g = 2.19$, $-2J = 61.53$ cm^{-1}, $\rho = 0.118$, and $R = [\sum(\chi_{obs} - \chi_{calc})^2/\sum(\chi_{obs})^2]^{1/2} = 6.9 \times 10^{-3}$.

Table 6. Magnetic Exchange Parameters and Distances of Copper Dimers

	$2J$ (cm^{-1})	Cu···Cu (Å)
$[Cu_2(Aden)_4(H_2O)_2]\cdot 6H_2O$[a]	−179	2.75
$[Cu_2(Aden)_4]\cdot 4H_2O$[b]	−257	2.95
$[Cu_2(Aden)_4(Cl)_2]Cl_2\cdot 6H_2O$[a]	−285	2.81
$[Cu_2(7\text{-Azaindole})_4\cdot 4DMSO$[c]	−389[d]	
$[Cu_2(stz)_4]$[e]	−61.5	2.67

[a] Reference 20. [b] Reference 15. [c] Reference 19. [d] The authors indicated that they are unable to distinguish whether both of the dimethyl sulfoxide (DMSO) molecules per copper are contained within the lattice or whether one of these is involved in axial coordination to copper. [e] This work.

Table 6 shows the magnetic exchange parameters in copper(II) complexes which exhibit pairwise exchange. From the table we can observe that the values of $-2J$ for the copper adenine complexes are higher than that for the $Cu_2(stz)_4$ complex, which is noteworthy because the Cu···Cu bond distance in this complex is the lowest. This is probably due to the effect of the axial ligand in the other complexes which affects the relative separation between the $d_{x^2-y^2}$ and d_{z^2} orbitals of the two copper(II) ions.[19] Sonnenfroh and Kreilick[20] found for the copper−adenine complexes that an increase in the axial bond distance signifies a decrease in the exchange energy value. In the $Cu_2(stz)_4$ complex there is not an axial ligand as a consequence because the value of $-2J$ is the lowest.

Molecular Orbital Calculations. In order to understand the reasons of the different values of the exchange energies between the copper−adenine complexes and the $Cu_2(stz)_4$ complex, we have performed molecular orbital calculations.

It is well-known that the interaction between two $S = {}^1/_2$ metal atoms in a dimer leads to two molecular states: a spin singlet ($S = 0$) and a triplet ($S = 1$) separated by $2J$. The interaction will be antiferromagnetic ($J < 0$) if $S = 0$ is the ground state; on the contrary if $S = 1$, the interaction will be ferromagnetic ($J > 0$). Whereas ferromagnetic contributions are usually small, antiferromagnetic ones can be considered as proportional to the square of the gap between the molecular orbitals constructed from the magnetic orbitals.[38] Extended Hückel molecular orbital (EHMO) calculations (atomic parameters used are given in Table 7) can be employed to evaluate such interactions. The EHMO calculations performed in this work have been made, by means of the CACAO program.[39] For a copper(II) dimer with one unpaired electron on each metal atom two molecular orbitals are generated from the combination of magnetic orbitals (symmetric and antisymmetric forms).

(35) Goodgame, D. M. L.; WAggett, S. V. *Biochem. Biophys. Res. Commun.* **1971**, *42*, 63.
(36) Bertini, I. *ESR and NMR of Paramagnetic Species in Biological and Related Systems*; Bertini, I., Drago, R. S., Eds.; Reidel: Dordrecht, The Netherlands, 1980.
(37) Otieno, T.; Rettig, S. J.; Thompson, R. C.; Trotter, J. *Inorg. Chem.* **1993**, *32*, 4384.
(38) Kahn, O. *Angew. Chem., Int. Ed. Engl.* **1985**, *24*, 834.
(39) Mealli, C.; Proserpio, D. Computer Aided Composition of Atomic Orbitals (CACAO program) PC version, July 1992. See also: *J. Chem. Educ.* **1990**, *67*, 399.

Table 7. Orbital Exponents (Contraction Coefficients in Double-ζ Expansion Given in Parentheses) and Energies Used in the Extended Hückel Calculations

atom	orbital	$\xi_i(c_i)$	H_{ii} (eV)
O	2s	2.275	−32.30
	2p	2.275	−14.80
N	2s	1.950	−26.00
	2p	1.950	−13.40
C	2s	1.625	−21.40
	2p	1.625	−11.40
H	1s	1.300	−13.60
S	3s	1.900	−20.30
	3p	1.900	−14.00
Cu	4s	2.200	−11.40
	4p	2.200	−6.06
	3d	5.950(0.5933)	−14.00
		2.300(0.5744)	

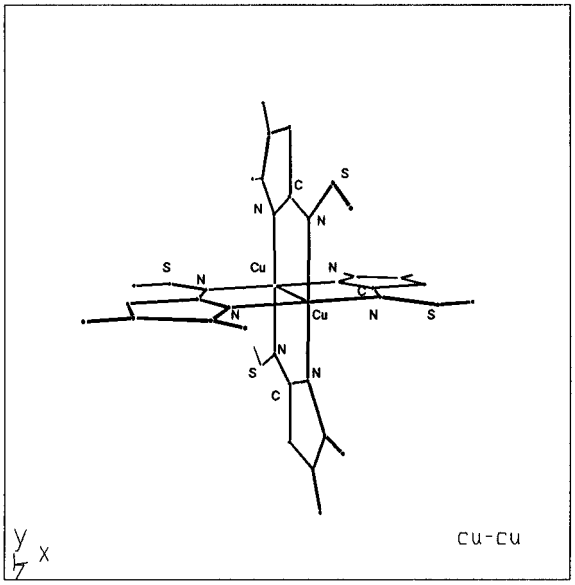

Figure 8. Idealized form of the $Cu_2(stz)_4$ complex.

Table 8. Energy of the $d_{x^2-y^2}$ and d_{z^2} Orbitals of the $Cu_2(stz)_4$ Model from the Variation of the Cu−L Axial Bond Distance

Cu−L bond distance	$E(d_{x^2-y^2})$	$E(d_{z^2})$
2.10	−10.664	−12.419
2.20	−10.664	−12.550
2.30	−10.664	−12.589
2.40	−10.664	−12.887
2.50	−10.664	−13.059
2.60	−10.664	−13.087
	−10.664	−13.152

With the aim of understanding the influence of the axial ligand, we calculate the variation of the energy of $d_{x^2-y^2}$ and d_{z^2} orbitals with respect to the Cu−L axial bond distance in one model for the $Cu_2(stz)_4$ complex being the Cu···Cu bond distance of 2.60 Å (see Figure 8). Table 8 shows the results of the calculation, where one can appreciate that the energy differences diminish when the Cu−L axial bond distance is shorted. These variations will affect the magnitude of the exchange interaction because the d_{z^2} orbital overlaps more efficiently and must be mixed with the $d_{x^2-y^2}$ orbital. These results are in agreement with that reported by Sonnenfroh and Kreilick. However, the axial bond distances observed in the copper−adenine complexes (from 2.20 to 2.43 Å) are rather long; as a consequence we suggest that the mixture of the $d_{x^2-y^2}$ and d_{z^2} orbitals must be small and that it is not the only factor that contributes to the differences of $-2J$ values.

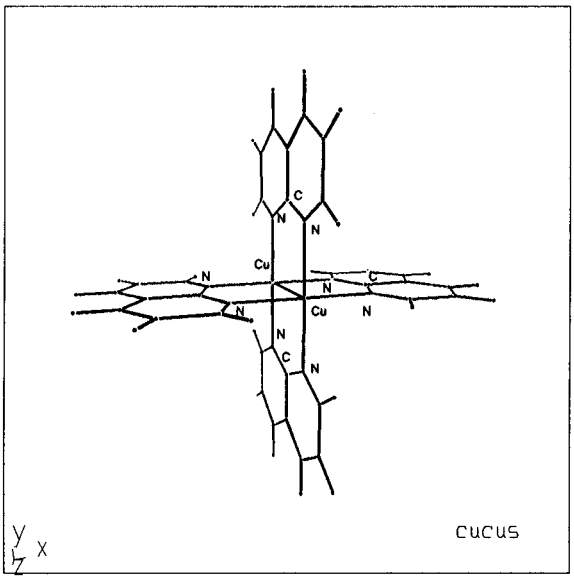

Figure 9. Idealized form of the copper−adenine complexes.

We have studied the influence of the bridging ligand nature, proposing another model for copper complexes with a NCN bridge (see Figure 9), where the selected Cu···Cu bond distance was 3.00 Å, which has been reported for one of the copper−adenine complexes.[19] The EH calculation program indicates that the SOMO's of the copper−adenine model has a difference of energy of 212 meV, while, for the copper−sulfathiazole one, the value is 104 meV. These results are according to the experimental values of the exchange energies observed in the Table 6. The difference could be explained from the most favorable electron transfer that takes place through the aromatic rings in the copper−adenine complexes.[15]

Acknowledgment. We thank Drs. F. Lloret (University of Valencia) and T. Rojo and L. Lezama (University of Pais Vasco) for their assistance in the magnetic and EPR measurements. We greatly appreciate financial support from the Comisión Interministerial de Ciencia y Tecnología (SAF 94-075). J.C. thanks the Generalitat Valenciana (Spain) for a Doctoral fellowship.

Supporting Information Available: Tables listing crystal data and structure refinement, atomic coordinates and equivalent isotropic displacement parameters, bond lengths and angles, hydrogen bonds, anisotropic displacement parameters, calculated hydrogen coordinates, isotropic displacement parameters, and torsion angles (14 pages). Ordering information is given on any current masthead page.

IC960968P